

© 2022 IEEE. Personal use of this material is permitted. Permission from IEEE must be obtained for all other uses, in any current or future media, including reprinting/republishing this material for advertising or promotional purposes, creating new collective works, for resale or redistribution to servers or lists, or reuse of any copyrighted component of this work in other works.

Electrodynamic models of combustion chamber with initiated sub-critical streamer discharge

P.V. Bulat¹, I.I. Esakov², P.B. Lavrov², A.A. Ravaev², K.N. Volkov³

¹Baltic State Technical University, 190005, St Petersburg, Russia

²Moscow Radiotechnical Institute of Russian Academy of Sciences, 117519, Moscow, Russia

³Kingston University, SW15 3DW, London, United Kingdom

Abstract

Various electrodynamic models of a combustion chamber are considered, in which an initiated subcritical streamer discharge is used to ignite a combustible mixture. To localize the discharge in the working chamber, initiators based on half-wave electromagnetic vibrators with resonant properties are used. The dependences of the structure of the electric fields forming the discharge on the geometric parameters of the discharge initiator are obtained, and the issues of matching the chamber with the radiation generator are considered. Comparison of the calculation options for different positions of the initiator of the discharge in relation to the optical axis of the camera. Possibilities for further enhancement of the field in the working zone at the poles of the microwave discharge initiator, which is required for the formation of discharges with a developed streamer structure at elevated gas pressures in the combustion chamber, are discussed. The ways of increasing the resulting electromagnetic field in the area of vibrators for the formation of discharges with a volumetric structure have been determined.

Keywords

microwave radiation, streamer discharge, combustion chamber, electrodynamic model, plasma-assisted combustion

Introduction

The use of initiated microwave discharges to ignite combustible mixtures in a high-pressure chamber makes it possible not only to create such discharges at a significantly lower power of the microwave energy source, but also to localize them in the working chamber in the right place [Bulat21iee]. Comparative studies of the ignition of a combustible mixture by a spark discharge from candles of a standard configuration and initiated microwave discharges were carried out in [Bulat21tpl]. Research results have shown that ignition with microwave discharge is energetically much more efficient than spark ignition [Bulat21jtp]. The combustible mixture is ignited by a microwave discharge, the better, the more branched system of plasma channels it has [Bulat19]. The results obtained are of interest for the creation and application of non-equilibrium microwave discharges for ignition and intensification of fuel combustion in high-speed flows [Shibkov09, Vinogradov19]. The results of theoretical and experimental studies of a combustion chamber based on an injection-type plasma combustion system are presented in [Matveev15].

The possibilities of using discharges of various types and non-equilibrium plasma to ignite fuel mixtures and various applications are discussed in [Rao10, Starikovskiy13, Ju15, Matveev19, Matveev21]. The properties of freely localized microwave discharges in a focused beam of quasi-optical radiation have been studied quite well [Aleksandrov92, Avramenko05]. Various approaches have also been developed to simulate the propagation of microwave radiation in waveguides with different cross-sectional shapes [Finnveden08, Kudryavtsev17]. The interaction of microwave radiation with low-temperature plasma is discussed in [Yao20].

The results of theoretical and experimental investigations of a developed synthesis gas

afterburner based on an injector type plasma-assisted combustion system are presented in [Matveev15]. The basic overall dimensions of the afterburner with the injecting device are determined. The design concept can provide higher performance, wider turndown ratios, more efficient synthesis gas combustion, and satisfaction of major ecological requirements. Combustion dynamics are investigated for plasma-enhanced methane-air flames in premixed and nonpremixed configurations using a transient arc dc plasmatron in [Rao10]. The results of the investigation of the possibilities to produce high volume and high concentration of nitrogen oxides in ICP/RF plasma for industrial application are presented in [Matveev19]. The results of modeling, design, and experimental investigation of a heat exchanger to be used downstream of a radio frequency plasma torch for a variety of applications are reported in [Matveev21]. The interaction of microwaves with low-temperature plasma in a plasma-metal model using the finite-difference time-domain (FDTD) method to simulate the scenarios of uniform, linear, parabola, and Epstein plasma distribution is studied in [Yao20].

To localize the discharge in the working chamber, initiators based on half-wave electromagnetic vibrators are used. The most well-studied type of microwave discharge initiator is the linear electromagnetic vibrator. Its advantages include the simplicity of the design, the well-known dependences of the field near the ends on various factors, as well as the possibility of ensuring the breakdown of the medium at high values of the sub-criticality index of the initial field. The theory and methods of calculating initiators of various designs are given in [Khodataev07]. The influence of conductivity, geometric dimensions and shape of the initiator and their groups on the local properties of induced electromagnetic fields are considered in [Grachev12].

The location of the initiator of the discharge near the metal shield or on the surface of the dielectric shield provides additional opportunities for field amplification. In this case, the initiator of the discharge is a piece of metal wire with rounded ends. In general, the smaller the tip radius and the closer the resonator is to the screen, the greater the field gain [Lebedev15]. In the case of a dielectric screen, the resonator is placed directly on its surface. The maximum field intensity in this case is observed in the space formed by the surface of the screen and the radius tip of the resonator [Bulat19]. Under resonance conditions, a large induced current arises in the conductor, and gas ionization occurs in the vicinity of the initiator, and plasma channels are formed that heat the surrounding gas.

The studies have shown that the installation of an electromagnetic vibrator at a small distance from the metal shield allows for air breakdown at a radiation power significantly lower than that required for breakdown in unlimited space [Esakov19] (deeply subcritical streamer discharge). In [Esakov09], an energetically efficient method of controlling the boundary layer is proposed by creating on the surface of the model a regular system of localized microwave discharges formed in the field of a quasi-optical electromagnetic beam of a remote microwave energy source.

The structure of microwave fields in a discharge chamber used to obtain an electrode discharge was investigated in [Lebedev11]. Numerical simulation makes it possible to quantitatively determine the details of the design of the discharge chamber, which are optimal for the generation of the discharge. The dependence of the structure of the electric fields forming the discharge on the geometric parameters of the discharge chamber is obtained, and the issues of matching the discharge system with the generator are considered.

As part of applied scientific research, a complex experimental setup was created as part of a powerful pulsed microwave generator and a high-pressure pipe, simulating a combustion chamber [Bulat21jtp]. The installation is equipped with a system for measuring pressure in the working chamber, which allows measuring both static pressure and the process of changing

pressure over time with a resolution of at least 1 ms. In addition, it is possible to register optical radiation from the working chamber through the longitudinal window.

In earlier experiments, microwave radiation was fed into the chamber using a flat rectangular horn through one of the side slots with a radio-transparent dielectric window. The same slit with a window on the opposite side of the tube was used for visual observation and photographing of the formed discharges. The pulse power of the used microwave radiation source is $P=500$ kW, the operating frequency is $f_0=2.795$ GHz (wavelength $\lambda=10.7$ cm), and the pulse duration is $\tau=2-6$ μ s.

The initiators were half-wave linear vibrators in the form of metal wire segments with rounded ends and were located on the camera axis and simultaneously parallel to the microwave radiation polarization vector. The results of studies carried out in [Bulat21jtp, Bulat21tpl, Bulat21ieee], have demonstrated the fundamental possibility of implementing and promising the use of microwave-discharge ignition systems in high-pressure combustion chambers. In this case, the initiated microwave discharges had the form of single streamers of limited length, which is explained by the short duration of the radiation source pulses. One of the ways to increase the efficiency of the studied microwave ignition systems at the same energy parameters of the microwave radiation source is the formation of discharges with a developed bulk streamer structure [Starikovskiy13, Ju15].

As a result of the research, the ways of increasing the resulting EM field in the area of vibrators for the formation of discharges with a volumetric structure have been determined. In particular, it was found that the well-known concepts of the classical EM vibrator and its properties in free space are inapplicable in the case of placing vibrators-initiators in the working chamber.

A classic half-wave EM vibrator made of a piece of metal wire with high conductivity, from an electrical point of view, is a high-quality resonant oscillatory circuit (LC-circuit). Capacitor C is a reactive element with the ability to store and release electrical energy. The inductor L is a reactive element that has the ability to store and release magnetic energy. After the formation of the discharge at the poles of the vibrator, the ohmic resistance of the plasma discharge channels is introduced into its equivalent resistance. The quality factor of the vibrator and the resulting electric field at the poles decrease, and the dynamics of the streamer discharge development slows down. This is true for an EM vibrator located far from any parts and structures at a distance of at least several wavelengths at the operating frequency.

This study considers the construction of a three-dimensional electrodynamic model of a microwave ignition system in a cylindrical combustion chamber, as well as the determination of the spatial distribution and amplitude of EM fields in the system both before and after the generation of the discharge. On the basis of the performed calculations, ways of increasing the resulting EM field in the region of vibrators for the formation of discharges with a volumetric structure are discussed.

Structure of discharge

An experimental verification of the possibility of initiating microwave discharges in a high-pressure pipe at an increased starting pressure has been performed. For this, an initiator with a resonance length of 53 mm was placed in the tube and a pressure of 1 to 4 bar was created, the microwave generator was turned on at a maximum power equal to 500 kW. The pulse duration was 6 μ s. The formation of a microwave discharge was visually observed. At all tested pressures, a microwave discharge was initiated, shown in Figure 1a. This confirms the possibility of the

formation of microwave discharges at elevated pressures. The maximum streamer size in this case is 5 mm.

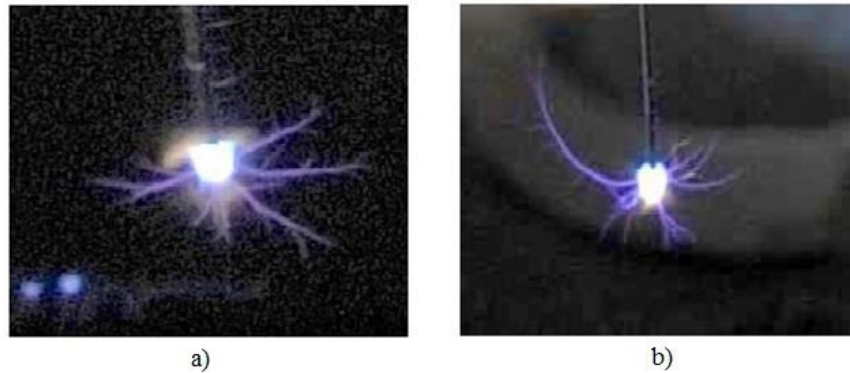


Fig. 1. Streamer discharge on initiator (a) and streamer discharge on initiator with horn antenna (b) for pressure 1 bar

To amplify the electromagnetic field in the area of the vibrator, a mock-up of a horn antenna with an aperture of 72×25 mm was developed and manufactured. The high-pressure tube also contained an initiator with a resonance length of 53 mm and a pressure of 1 bar. The discharge was initiated at the same microwave parameters as in the absence of a horn antenna. A photograph of the microwave discharge is shown in Figure 1b. The maximum streamer size in this case is 10 mm.

The experience of working with microwave discharges in gases at atmospheric and elevated pressures in free space shows that the developed structure of the discharge can be realized with a further increase in the electric field exciting the discharge at the poles of the EM vibrator [Bulat21ieee]. In this case, the nature and degree of change in the resulting EM field at the vibrator poles during the development of the discharge are of great importance.

Microwave radiation input to the chamber

From a physical point of view, there are two different approaches to creating a microwave ignition system in a working chamber: the location of the EM vibrator perpendicular to the optical axis of the chamber and parallel to it with a corresponding change in the field polarization and the design of the EM radiation input into the chamber.

1. Model with a vibrator perpendicular to the optical axis of the chamber

In variant 1 of the design of the microwave ignition system, the vibrator is located perpendicular to the optical axis of the working chamber. Due to the polarization of the radiation (the vector E is parallel to the axis of the linear vibrator), there are only two options for inputting radiation into the chamber: input using a flat horn or flat waveguide through a side longitudinal window in the camera. Option 2 uses a vibrator located parallel to the optical axis of the camera.

A model of a working chamber with a horn input of microwave radiation is shown in Figure 2. The model uses a purely electrodynamic program technique, which is usual for such structures: the walls of the chamber, flanges and other metal elements are absent as unnecessary, since an ideal conductor is assumed under the outer space. The model contains only the internal parts of the structure, which are seen by the electromagnetic wave. The electrodynamic model includes areas with a dielectric constant equal to unity (vacuum) and side windows made of plexiglass (polymethyl methacrylate). The vibrator is a piece of metal wire with rounded ends.

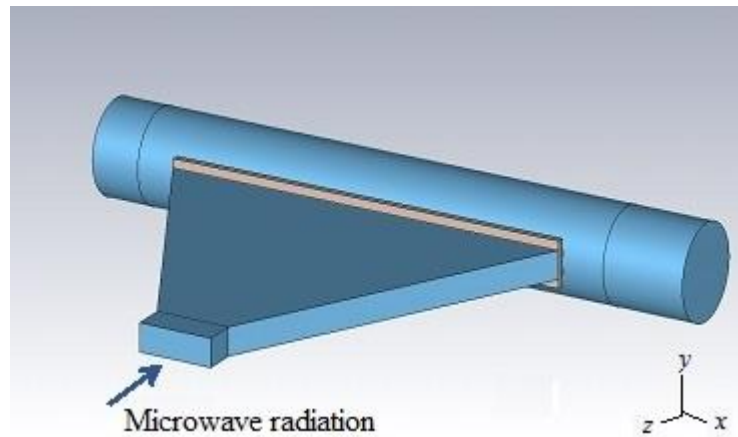


Fig. 2. Horn input of microwave radiation

One of the ways to increase the field in the vibrator region is to replace the horn with a regular waveguide with the concentration of the microwave energy flux near the output aperture of the waveguide.

2. Model with a vibrator parallel to the optical axis of the chamber

In variant 2 of the design of the microwave ignition system, the vibrator is located parallel to the optical axis of the working chamber. In this case, only the supply of microwave energy from the side of the chamber with a 90-degree rotation of the waveguide has a physical meaning. To determine the possibility and prospects of using such a design option at a qualitative level, a simplified model of the system without dielectric windows, a second window and other structural elements of the system is considered. The appearance of the electrodynamic model is shown in Figure 3. The initial inner diameter of the chamber in the model corresponded to the design and was 85 mm. The section of the waveguide path is $72 \times 34 \text{ mm}^2$. There is a polarization of radiation parallel to the optical axis of the camera and simultaneously to the axis of the linear EM vibrator.

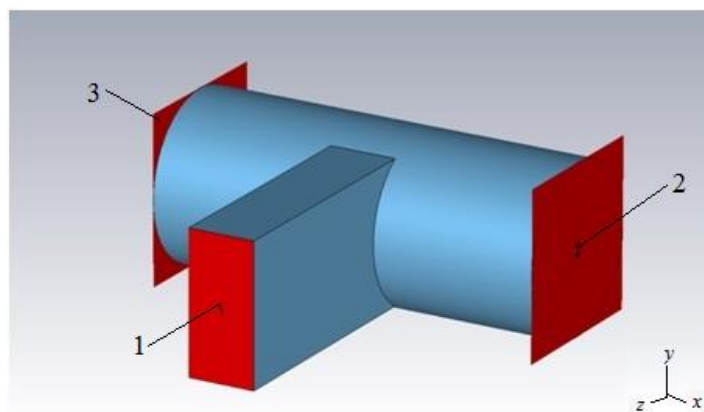


Fig. 3. Waveguide input of microwave radiation when linear electromagnetic vibrator is parallel to optical axis of the chamber

Through the waveguide port 1, radiation enters the chamber. At the ends of the chamber there are coordinated receiving ports 2 and 3. In other words, there is no reflection of radiation at the ends of the chamber, therefore the length of the cylindrical chamber should be at least $2\lambda \sim 200 \text{ mm}$. Further increase in the length of the chamber in the considered model has no physical meaning.

Mathematical model

To find the distribution of the electric field strength vector at the operating frequency, Maxwell's equations are solved, written in frequency-dependent form, inside the discharge chamber with conducting walls of all constituent parts of the structure. In the plane through which the radiation enters the system, in all calculations, a transverse electromagnetic wave (TEM) is excited at the operating frequency f_0 at a given input signal power. Considering that the losses at the boundaries of the region, the losses are small in relation to other losses in the system, the PEC boundary condition is used.

The tangential components of the vectors of the strength of the electric and magnetic fields at the interface between the two media are continuous. When studying an alternating electromagnetic field outside metal conductors, at the interface with the metal, the conductors are often replaced by a perfectly conducting medium. This replacement is based on the fact that an ideally conducting medium reproduces quite correctly the effect of real metal conductors on the electromagnetic field outside them.

To solve the basic equations of electrodynamics, the Finite Element Method (FEM) is used, which includes adaptive generation and division of mesh cells. Solutions for the electromagnetic field, found from Maxwell's equations, make it possible to accurately determine all the characteristics of a microwave device, taking into account the occurrence and transformation of some types of waves into others, losses in materials and radiation, etc.

The distribution of the electromagnetic field in the waveguide is determined by the type of wave and the nature of the load on the waveguide. If the length of the waveguide is infinitely large or it is loaded with an ideally absorbing load, then only the wave propagating from the field source propagates along the waveguide. A non-absorbing (reactive) load in the form of a section of a waveguide closed at the end causes a complete reflection of the wave propagating from the source. As a result of the addition of two counter propagating waves, incident on the load and reflected from it, a standing wave is established in the waveguide. For a standing wave, in contrast to a travelling one, there are times when either an electric or a magnetic field is absent in the waveguide. The energy is completely converted into the energy of the electric field or into the energy of the magnetic field.

In the waveguide, waves of electrical E_{mn} and magnetic H_{mn} types can propagate. The subscripts m and n are related to the distribution functions of the amplitudes along the transverse coordinates x and y . Each pair of numbers m and n in a particular design corresponds to a certain structure of the electromagnetic field and the value of the critical wavelength.

For periodic amplitude distribution functions, the index m determines the number of field half-periods that fit along the wide wall of the waveguide. Index n determines the number of field half-periods that fit along the narrow wall of the waveguide. The indices m and n can take any values, except for $m=0$ and $n=0$ for both types of waves. For an electric type wave E_{mn} , the electric field strength vector has a longitudinal component E_z , which coincides with the direction of propagation, and transverse components, and the magnetic field strength vector has only transverse components. For a wave of the H_{mn} type, the vector of the magnetic field strength has longitudinal and transverse components, and the vector of the electric field strength has only transverse components.

Results and discussion

1. A variant with an initiator positioned perpendicular to the optical axis of the chamber and a horn input of microwave radiation.

Before modelling the ignition system in the complex, it is required to determine the presence and degree of influence on the initial structure of the EM field in the system of various kinds of inhomogeneities and elements of the real structure of the chamber (its windows with dielectric inserts, "short-circuiting" of the chamber pipe on the right and the viewing dielectric window on the left, steps at the ends of the pipe and etc.).

The distributions of the electric field strength along the x and z axes are shown in Figure 4 for a camera with one viewing window (line 1). The presence of any irregularities in the working area leads to a significant change in the distribution of fields in the chamber. As an example, Figure 4 shows the changes in the electric field amplitude on the optical axis of the chamber tube x and along the horn axis z (the z coordinate is measured from the wall of the chamber tube opposite to the horn) when a second viewing window is introduced from the side opposite to the horn and at the same time dielectric inserts made of polymethyl methacrylate are installed in the windows (lines 2). Plexiglas inserts are used to separate the working volume of the high-pressure combustion chamber from the external environment and the waveguide path. There are not only abrupt changes in the field distribution, but also a periodic structure characteristic of a standing wave on the right side of the graphs near the pipe shorting on the right (Figure 4a) and a similar view of the field graphs in the horn and waveguide (Figure 4b).

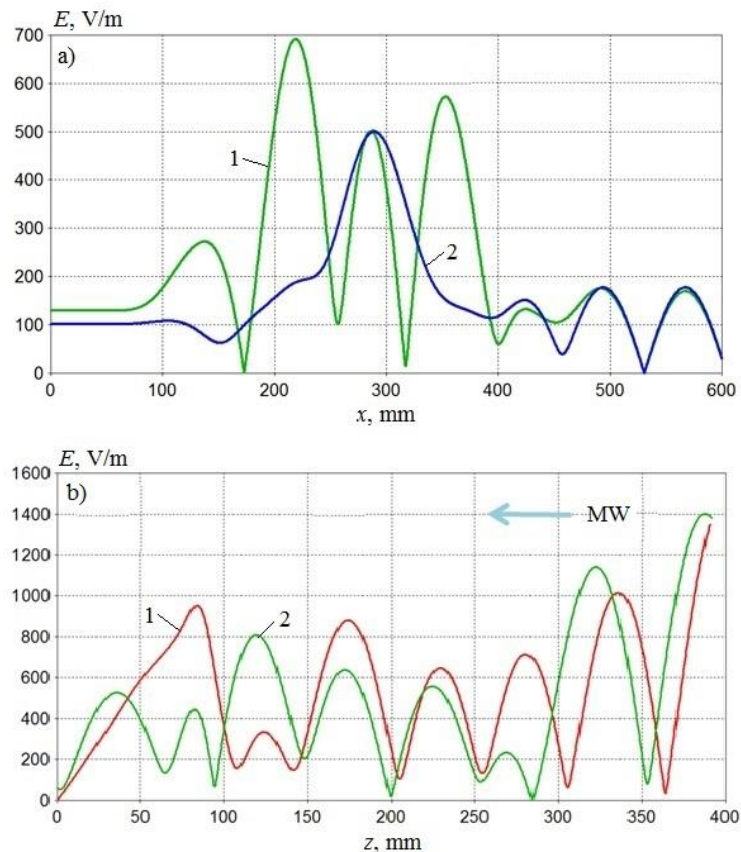


Fig. 4. Distributions of electric field strength in x (a) and z (b) directions. Lines 1 correspond to the combustion chamber with one observation window and lines 2 correspond to the case with the second observation window on the side opposite to the horn

The distributions shown in Figure 4 indicate a substantially non-uniform axial distribution of the field in the model under consideration and its strong difference from the classical cosine distribution of the field in a plane rectangular waveguide excited at the lowest type of wave H_{10} .

The diagram of the electric component of the EM field in a real structure in the section $y=0$ is

shown in Figure 5. The specified features of the propagation of EM waves in the system, including the spotty nature of the field, indicate the excitation of higher types of waves in the chamber and strong reflection of microwave radiation in the path. Strong reflection of radiation in the investigated design of the ignition system and the working chamber is a characteristic feature of the considered methods of microwave energy input from the side and perpendicular to the chamber axis.

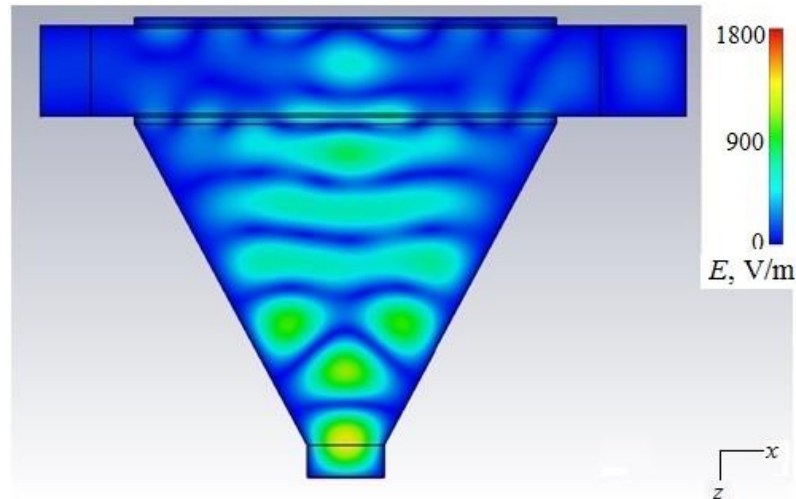


Fig. 5. Initial distribution of electric field strength for $y=0$ without electromagnetic vibrator

Installing a half-wave electric vibrator-initiator of a microwave discharge in the chamber leads to a redistribution of EM fields in the system.

Development and experimental studies of the microwave ignition system are carried out at a fixed radiation frequency $f_0=2.795$ GHz. However, in the course of studying EM fields in model electrodynamic systems similar to the one under consideration, it is convenient to present the results obtained not only in space, but also in a certain frequency range. This allows you to visually describe the amplitude-frequency characteristics of the system and predict the impact of certain changes in it.

In Figure 6a shows a family of frequency dependences of the field amplitude at the poles of the EM vibrator at different vibrator lengths $L_v=45-50$ mm in the frequency range 2.4–3.2 GHz. For convenience, the results obtained are shown in a narrower frequency range - near the operating frequency (Figure 6b). In all considered cases, the diameter of the vibrator is 1 mm.

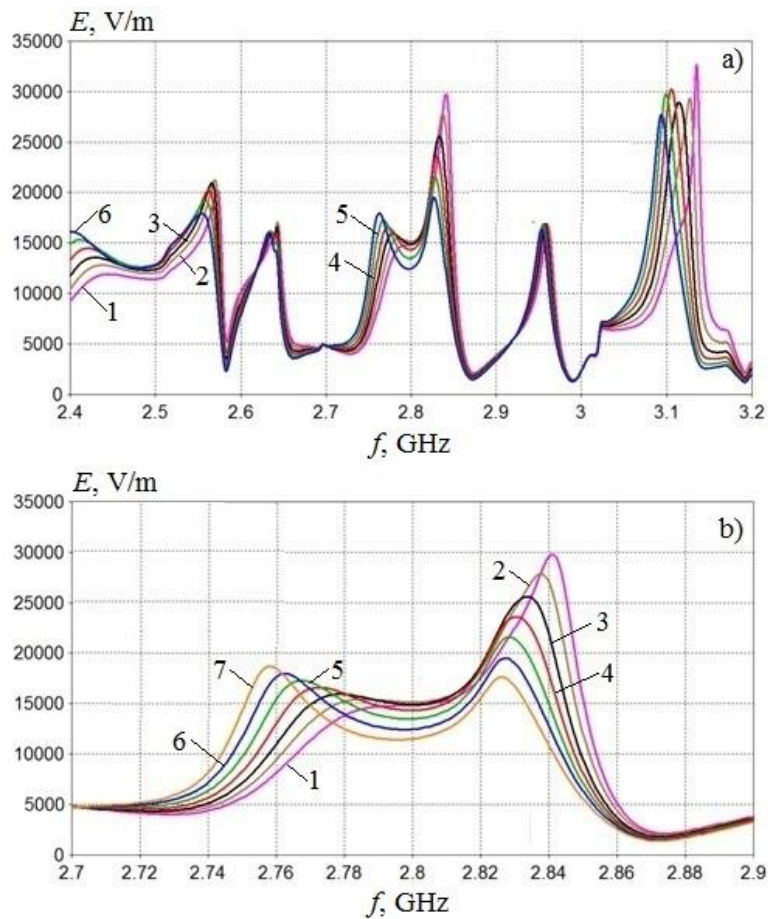


Fig. 6. Distributions of amplitude of electric field strength on vibrator poles for various vibrator lengths in wide (a) and narrow (b) frequency interval for the reduced on 120 mm length of the chamber for $L_v=45$ mm (1); 46 mm (2); 47 mm (3); 48 mm (4); 49 mm (5); 50 mm (6); 51 mm (7)

The values of the EM field indicated in the graphs correspond to the normalized value of the microwave power at the input to the system, equal to 1 W. To estimate the true amplitude of the electric field at the desired point, it is sufficient to multiply the value shown in the graph by the square root of the ratio of the real radiation power at the input of the system to the normalized value of 1 W. So, for example, when the power of the microwave radiation source is 500 kW, the square root of this ratio is approximately 707, and the field amplitude on the graph 10^4 V/m corresponds to the real field value in the usual units $E \approx 70$ kV/cm.

The amplitude of the microwave electric field at which the electrical breakdown of air and most real combustible mixtures is observed at atmospheric pressure is approximately 30 kV/cm [Bulat21ieee]. Thus, over the entire range of values of the vibrator length of practical interest at an operating frequency of 2.8 GHz, the pulse amplitude of the electric field at the vibrator poles is more than sufficient for gas breakdown not only at atmospheric, but also at increased pressure in the chamber even under initial conditions (without any optimization of the geometry and dimensions of the system).

An important feature that you need to pay attention to when analyzing the graphs in Figure 7, consists in the multi-resonant nature of the EM field in the system on the frequency axis, which is fundamentally different from the usual form of the resonance curve of a half-wave vibrator in free space (bell-shaped curve). Unlike an EM vibrator in free space, its length in the interval of interest has little effect both on the field amplitude at the poles and on the characteristics of the system as a whole.

From an electrical point of view, the system under consideration with a vibrator is not a single LC circuit, but a system of coupled circuits with their resonances determined by a set of system parameters - the diameter and length of the working chamber, the shape and dimensions of the windows in the chamber, the dimensions and permeability of dielectric inserts in the windows. and, of course, the size and location of the EM vibrator in the chamber. This feature of the studied electrodynamic system practically excludes the possibility of its usual tuning by changing the geometric dimensions of the vibrator. The entire structure needs to be tuned and optimized.

The microwave field diagram in a system with a vibrator in the section $y=0$ is shown in Figure 7. At the location of the vibrator (indicated by a cross in the figure) near its centre, the amplitude of the electric field at a given polarization is equal to zero.

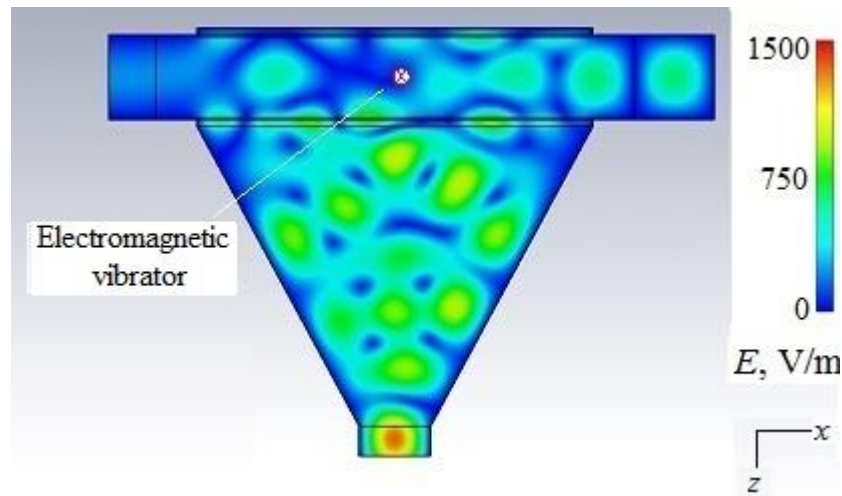


Fig. 7. Distribution of electric field strength for $y=0$ in the chamber with electromagnetic vibrator

Another important issue is to determine possible changes in the amplitude of the EM field at the vibrator poles after the onset and development of a streamer microwave discharge. The construction of an accurate physical model of a vibrator with a developed volume discharge is hardly possible and justified from the point of view of the time spent on modelling due to the structure, dimensions, and other parameters of the discharge continuously varying in time, as well as the lack of accurate data on the conductivity of individual structural elements of the discharge. A reasonable way out for qualitative analysis and quantification of the discharge model is to replace the Perfect Electric Conductor (PEC) with a finite conductive metal.

The equivalent conductivity of a streamer microwave discharge during development can vary over a wide range, as a result of which the effective resistance of the equivalent LCR circuit also changes (under R is remembered as a resistor element). The required range of changes in the conductivity of an EM vibrator with a length of $L_v \sim 5$ cm and a diameter of 1 mm is determined based on the range of change in the equivalent resistance of such a circuit, which is of real physical interest (Table 1).

Table 1. Equivalent resistance and conductivity of the vibrator

Equivalent resistance, Ohm	Conductivity, Cm/m
1	10^5
10	10^4
1000	10^3
1000	10^2

The corresponding graphs of the dependence of the field amplitude at the vibrator poles with the one selected in Figure 6 with length $L_v=48$ mm are shown in Figure 8. In this series of calculations, the length of the pipe was again increased by 57 mm to the actual dimensions and by 70 mm of its right section with a short circuit at the end. The drops in the $E(f)$ curves in the central part became sharper, but the dip and amplitude near the operating frequency $f_0=2.795$ GHz changed insignificantly. The influence of the vibrator conductivity (equivalent resistance of the streamer discharge plasma), as well as the vibrator length, in Figure 8 is also not essential.

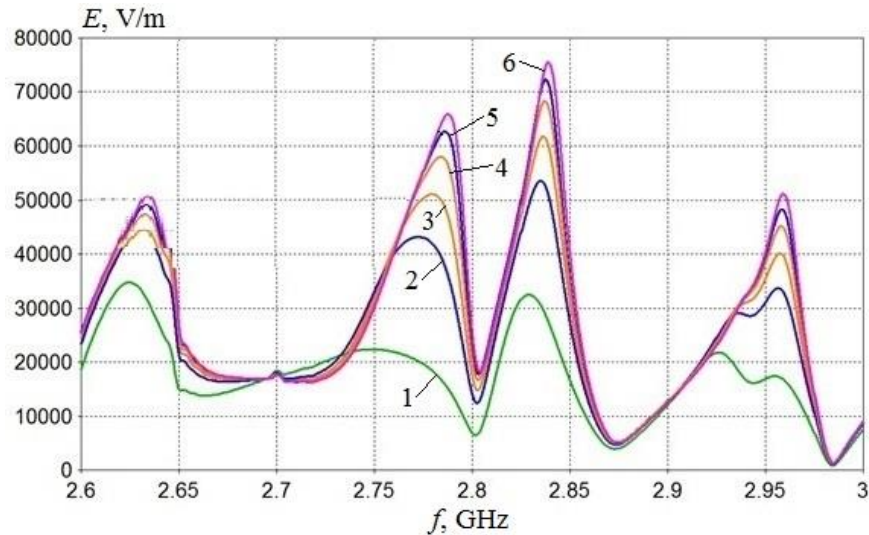


Fig. 8. Distributions of electric field strength on vibrator poles for vibrator length $L_v=48$ mm and various electric conductivities of the vibrator $\sigma=10^2$ Cm/m (1); 10^3 Cm/m (2); $3 \cdot 10^3$ Cm/m (3); 10^4 Cm/m (4); $3 \cdot 10^4$ Cm/m (5); 10^5 Cm/m (6)

A family of graphs of the parameter $S_{1,1}$ (reflection coefficient) of the same model is shown in Figure 9. Parameter $S_{1,1}$ is the field reflectance of radiation at the entrance to the system. In this case, at the operating frequency, $S_{1,1}=0.7-0.8$. The energy reflection coefficient in terms of power is still a characteristic of the entire system, and not of a separate vibrator in front of the horn aperture, and at the frequency f_0 this coefficient exceeds the value $(S_{1,1})^2 \geq 0.5$.

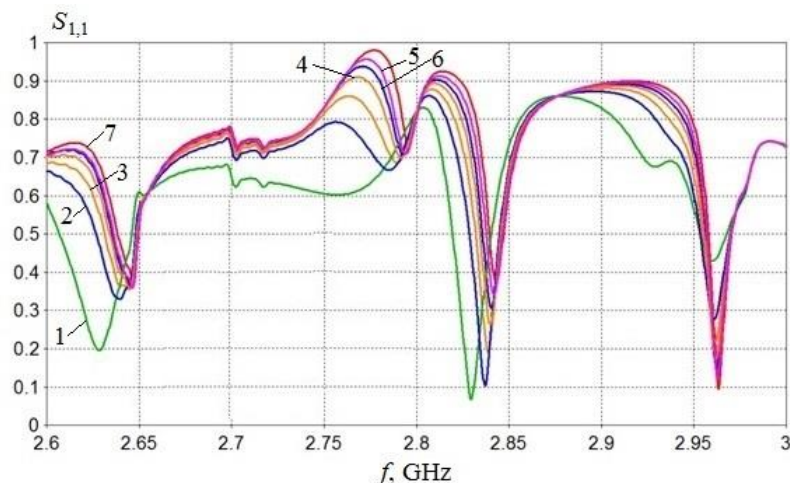


Fig. 9. Distributions of $S_{1,1}$ parameter in the waveguide of microwave radiation input for vibrator length $L_v=48$ mm and various electric conductivities of the vibrator $\sigma=10^2$ Cm/m (1); 10^3 Cm/m (2); $3 \cdot 10^3$ Cm/m (3); 10^4 Cm/m (4); $3 \cdot 10^4$ Cm/m (5); 10^5 Cm/m (6). Line 7 corresponds to PEC

Diagrams of the electric field distribution in two sections of the model at $y=0$ and $x=0$ with a vibrator conductivity $\sigma=10^3$ Cm/m (the equivalent resistance is 100 Ohm) are shown in Figure

10. In comparison with the diagram shown in Figure 7, changes in the field distribution in Figure 10 are extremely insignificant. The lower diagram also illustrates a sharp increase in the resulting field in the area of the vibrator near its poles.

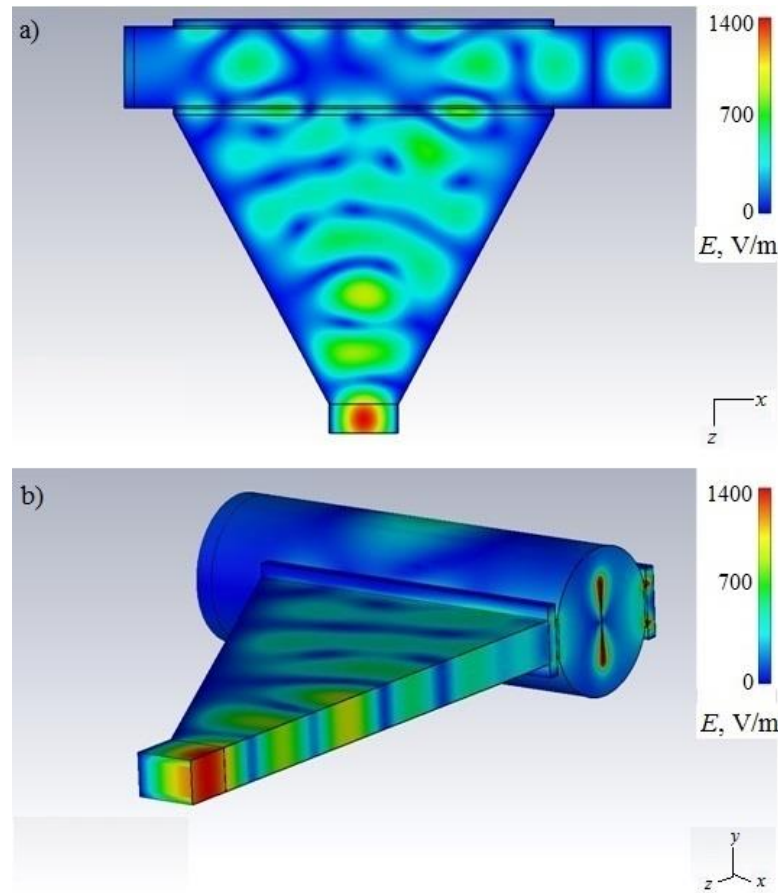


Fig. 10. Distributions of electric field strength for $y=0$ (a) and $x=0$ (b) with electromagnetic vibrator length $L_v=48$ mm and electric conductivity $\sigma=1000$ Cm/m

As in the previous case, a standing wave is formed in the system, and it is not possible to achieve a pure travelling wave regime. However, after the onset and development of a streamer discharge, the field amplitude at the vibrator poles and, obviously, at the streamer ends does not fall as fast as in the case of an EM vibrator in free space. In other words, the formation and development of the streamer volumetric structure of the discharge during the microwave pulse should proceed at an almost unchanged rate. To form a volumetric streamer microwave discharge, it remains only to find a way to increase the electric field at the poles of the EM vibrator.

2. Option with initiator location perpendicular to the optical axis of the camera and waveguide input of microwave radiation.

Families of curves of the amplitude of the electric field at the poles of the EM vibrator and the parameter $S_{1,1}$ at different lengths of the vibrator are shown in Figure 11, and similar dependences for the optimal length of the EM vibrator $L_v=45$ mm and different values of its conductivity are shown in Figure 12. The obtained frequency dependences retain, albeit less pronounced, but still the same multi-resonance character, formed by an equivalent system of coupled circuits with distributed parameters L and C .

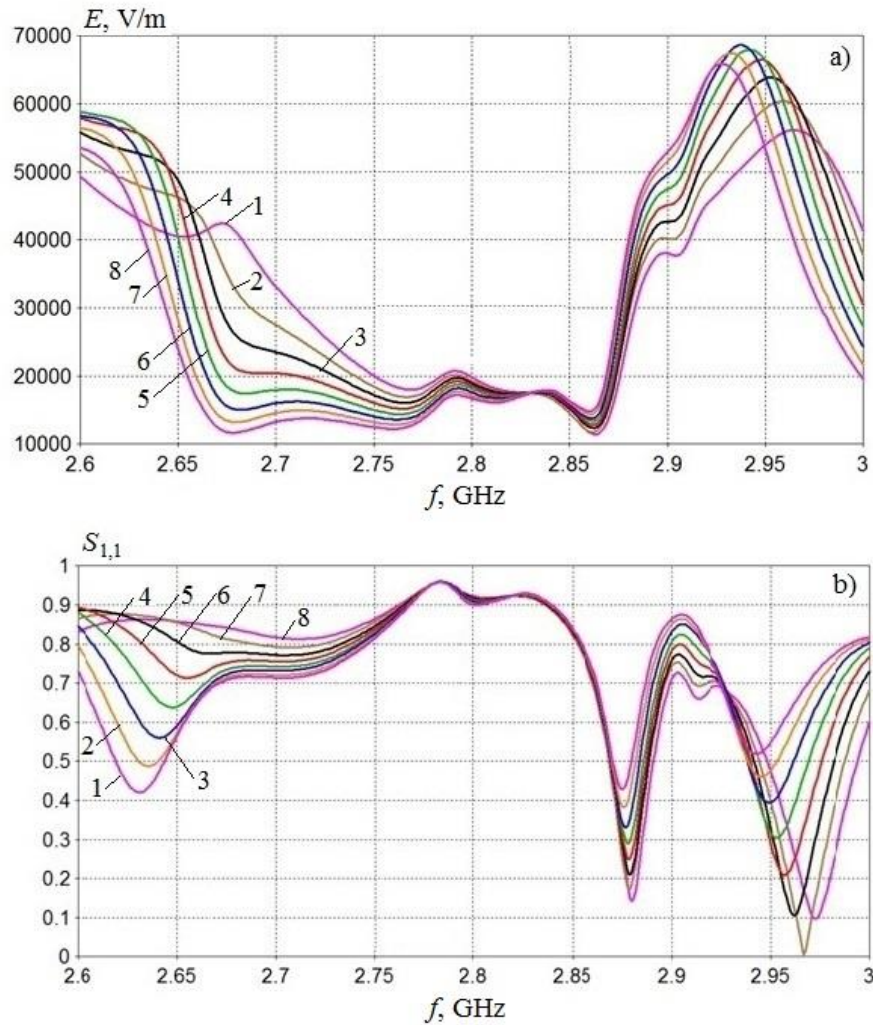


Fig. 11. Distributions of electric field strength on vibrator poles (a) and $S_{1,1}$ parameter (b) waveguide microwave radiation input for $L_v=45$ mm (1); 46 mm (2); 47 mm (3); 48 mm (4); 49 mm (5); 50 mm (6); 51 mm (7); 52 mm (8)

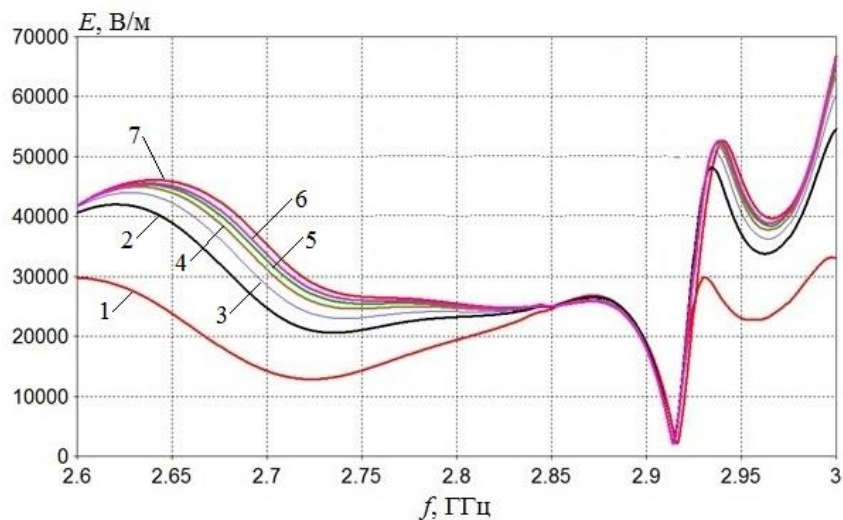


Fig. 12. Distributions of electric field strength on vibrator poles (a) and $S_{1,1}$ parameter (b) waveguide microwave radiation input for $L_v=45$ mm and various electric conductivities $\sigma=10^2$ Cm/m (1); 10^3 Cm/m (2); $3 \cdot 10^3$ Cm/m (3); 10^4 Cm/m (4); $3 \cdot 10^4$ Cm/m (5); 10^5 Cm/m (6). Line 7 corresponds to PEC

The reflection coefficient of microwave radiation in the input waveguide path is higher in power

and exceeds 80%. The influence on the characteristics of the system of parameters of the vibrator itself is still small. In the version of the system with a waveguide supply of microwave energy, the field amplitude at the operating frequency in conventional units is about 2×10^4 V/m, and with a power in the input path of 500 kW it reaches 140 kV/cm. With such an electric field strength and given vibrator parameters, it is possible to generate a microwave discharge at a gas pressure in the chamber $p=4$ ata or more.

At the same time, due to the highly non-uniform distribution of the field on the camera axis near the horn aperture (in comparison with the uniform cosine distribution) and the amplification of the amplitude in its central part, the gain from the use of waveguide input of microwave radiation is not as great as might be expected.

The presence of a clearly pronounced standing wave mode in the channel and the formation of an inhomogeneous field on the chamber axis is confirmed by the data shown in Figure 13 diagrams of the EM field in two sections of the model, $x=0$ and $y=0$ (a non-linear scale is used).

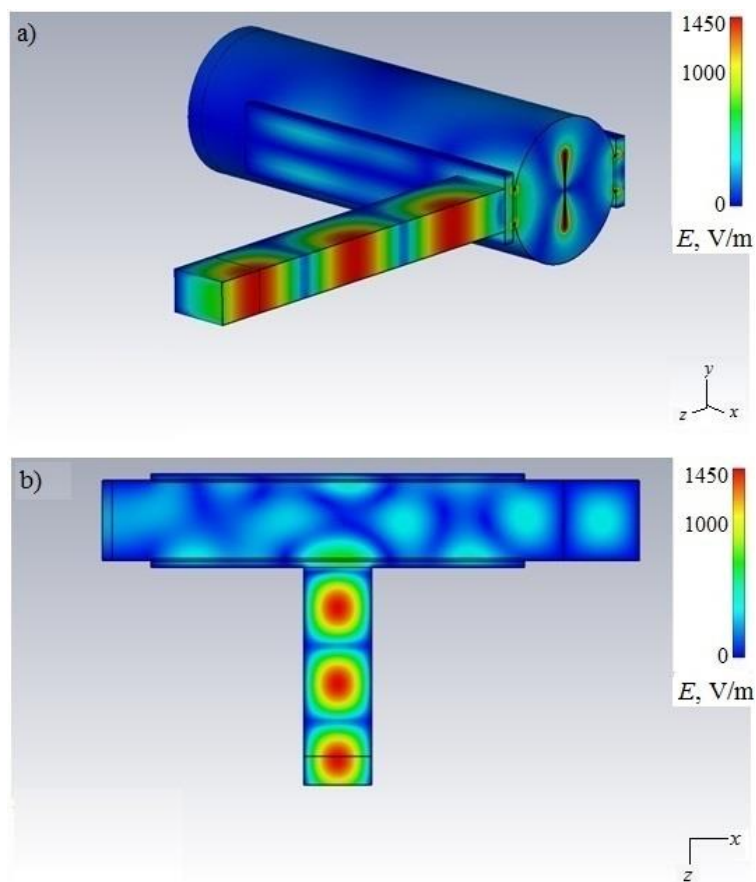


Fig. 13. Distributions of electric field strength for $y=0$ (a) and $x=0$ (b) with electromagnetic vibrator length $L_v=48$ mm and electric conductivity $\sigma=1000$ Cm/m

Attempts to further tune and improve the characteristics of the system by displacing the vibrator along the z-axis by the value s in the range from -30 to $+30$ mm were unsuccessful (Figure 14). The resulting families of curves (E_A and $S_{1,1}$ parameters) are even more rugged, and no gain in the field amplitude at the poles of the EM vibrator has been obtained.

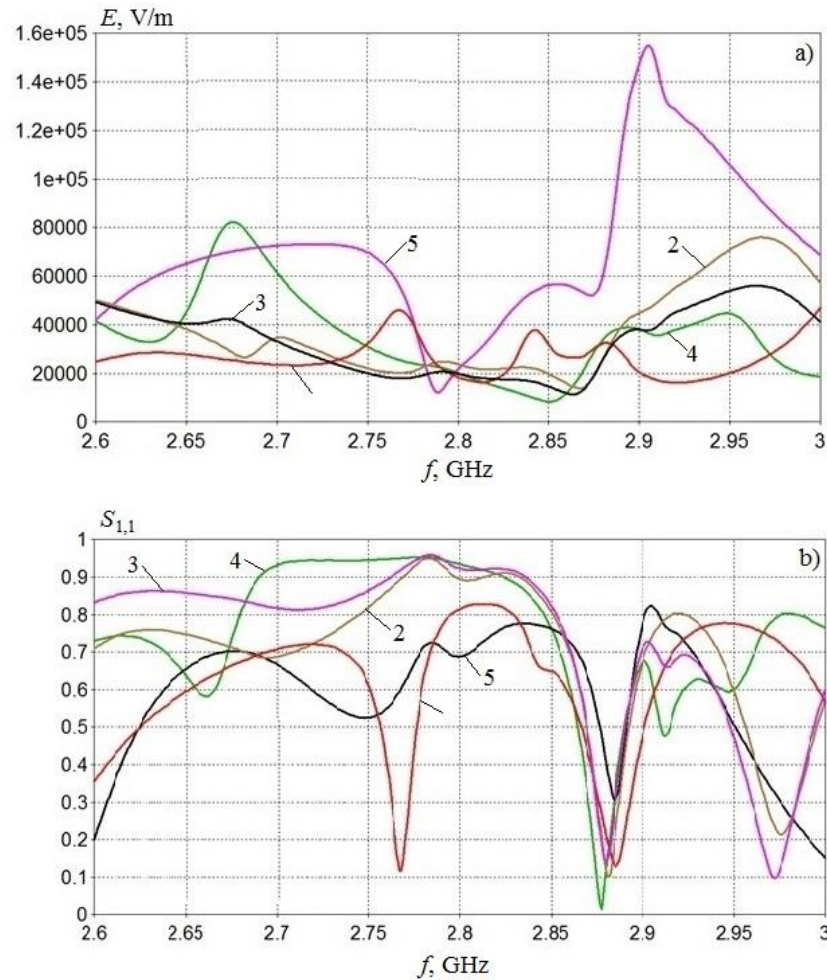


Fig. 14. Distributions of electric field strength on vibrator poles (a) and $S_{1,1}$ parameter (b) for vibrator length $L_v=45$ mm and various vibrator shifts from centreline $s=-30$ mm (1); -10 mm (2); 0 mm (3); $+15$ mm (4); $+30$ mm (5)

Conclusion

Simulation and detailed comparison of a number of methods of practical interest for the formation of initiated microwave discharges with a developed volumetric structure at a limited duration of EM radiation pulses have been performed. The results obtained confirm the possibility and prospects of using new efficient ignition systems in high-pressure combustion chambers based on initiated microwave discharges with a developed volumetric structure. Of greatest interest is the option of placing EM vibrators in the working chamber parallel to its axis with a corresponding change in the input of microwave radiation and the design of the chamber.

The results obtained are important for studying the effect of microwave discharges of various types on the combustion characteristics of a propane-air gas mixture at elevated pressure.

Before making a final decision on the issue of modification or radical modernization of the working chamber with an ignition system, it seems necessary to study and determine the possibility of using other designs of discharge initiators, in particular, quarter-wave vibrators with a base on the wall of the working chamber and a pole in its central part; ring vibrators with a cut, excited by the magnetic component of the microwave EM field; curvilinear initiators in the form of an arc segment, located near the walls of the cylindrical chamber with the introduction of microwave radiation from the end of the chamber.

Acknowledgements

This work was financially supported by the Ministry of Science and Higher Education of Russian Federation during the implementation of the project "Creating a leading scientific and technical reserve in the development of advanced technologies for small gas turbine, rocket and combined engines of ultra-light launch vehicles, small spacecraft and unmanned aerial vehicles that provide priority positions for Russian companies in emerging global markets of the future", No. FZWF-2020-0015.

References

1. [Bulat21ieee]P.V. Bulat, I.I. Esakov, L.P. Grachev, K.N. Volkov, I.A. Volobuev, "Experimental study of air breakdown induced by subcritical streamer microwave discharge", *IEEE Transactions on Plasma Science*, vol. 49, no. 3, pp. 1041–1049, 2021.
2. [Bulat21tpl]P.V. Bulat, K.N. Volkov, L.P. Grachev, I.I. Esakov, P.B. Lavrov, N.V. Prodan, P.S. Chernyshov, "Comparison of the energy efficiency of ignition of a fuel/air mixture by spark and streamer discharges", *Technical Physics Letters*, vol. 47, no. 15, pp. 51-54, 2021.
3. [Bulat21jtp]P.V. Bulat, K.N. Volkov, L.P. Grachev, I.I. Esakov, P.B. Lavrov, "Ignition of a fuel mixture using a multipoint pulsed spark discharge under various initial conditions", *Technical Physics*, vol. 66, no. 9, pp. 1308-1316, 2021.
4. [Bulat19]P.V. Bulat, L.P. Grachev, I.I. Esakov, A.A. Ravaev, L.G. Severinov, "Microwave breakdown of air initiated by an electromagnetic vibrator placed on a dielectric surface", *Technical Physics*, vol. 89, no. 7, pp. 957–961, 2019.
5. [Shibkov09]V.M. Shibkov, A.A. Aleksandrov, V.A. Chernikov, A.P. Ershov, L.V. Shibkova, "Microwave and direct-current discharges in high-speed low: fundamentals and application to ignition", *Journal of Propulsion and Power*, vol. 25, no. 1, pp. 123–137, 2009.
6. [Vinogradov19]V.A. Vinogradov, D.V. Komratov, A.Yu. Chirkov, "The effect of microwave discharge on subsonic gas flow with different power characteristics", *Journal of Physics: Conference Series*, vol. 1370, 012022, 2019.
7. [Matveev15]I.B. Matveev, S.I. Serbin, V.V. Vilkul, N.A. Goncharova, "Synthesis gas afterburner based on an injector type plasma-assisted combustion system", *IEEE Transactions on Plasma Science*, vol. 43, no. 12, pp. 3974-3978, 2015.
8. [Starikovskiy13]A. Starikovskiy, N. Aleksandrov, "Plasma-assisted ignition and combustion", *Progress in Energy and Combustion Science*, vol. 39, pp. 331–368, 2013.
9. [Ju15]Y. Ju, W. Sun, "Plasma assisted combustion: dynamics and chemistry", *Progress in Energy and Combustion Science*, vol. 48, pp. 21–83, 2015.
10. [Matveev19]I.B. Matveev, S.I. Serbin, "Synthesis of nitrogen oxides in ICP/RF plasma", *IEEE Transactions on Plasma Science*, vol. 47, no. 1, pp. 47–51, 2019.
11. [Matveev21]I.B. Matveev, S.I. Serbin, A.E. Zinchenko, "A high-temperature quenching reactor", *IEEE Transactions on Plasma Science*, vol. 49, no. 3, pp. 984–989, 2021.
12. [Rao10]X. Rao, S. Hammack, T. Lee, C. Carter, I.B. Matveev, "Combustion dynamics of plasma-enhanced premixed and nonpremixed flames", *IEEE Transactions on Plasma Science*, vol. 38, no. 12, pp. 3265–3271, 2010.
13. [Aleksandrov92]A.F. Aleksandrov, A.A. Kuzovnikov, V.M. Shibkov, "Freely localized shf discharge in a focused beam", *Journal of Engineering Physics and Thermophysics*, vol. 62, no. 5, pp. 519–525, 1992.
14. [Avramenko05]V.B. Avramenko, "Prebreakdown stage of a surface discharge fired by a pulse in the air at atmospheric pressure", *Journal of Engineering Physics and Thermophysics*, vol. 78, no. 1, pp. 187–195, 2005.
15. [Finnveden08]S. Finnveden, "Waveguide finite elements for curved structures", *Journal of Sound and Vibration*, vol. 312, pp. 644–671, 2008.

16. [Kudryavtsev17]I.V. Kudryavtsev, O.B. Gotselyuk, E.S. Novikov, V.G. Demin, “Specific features of waveguide heating due to transmission of high-power microwave signals”, *Technical Physics*, vol. 87, no. 1, pp. 101-106, 2017.
17. [Yao20]J. Yao, Z. Yu, C. Yuan, Z. Zhou, X. Wang, A.A. Kudryavstev, “The influence of plasma distribution on microwave reflection in a plasma-metal model”, *IEEE Transactions on Plasma Science*, vol. 48, no. 2, pp. 359–363, 2020.
18. [Khodataev07]K.V. Khodataev, “Various types of initiators for attached undercritical MW discharge ignition”, *AIAA Paper*, no. 2007-0431, 2007.
19. [Grachev12]L.P. Grachev, I.I. Esakov, P.B. Lavrov, A.A. Ravaev, “Induced field of an electromagnetic vibrator above a conducting screen placed in a microwave beam”, *Technical Physics*, vol. 82, no. 2, pp. 233–235, 2012.
20. [Esakov09]I. Esakov, L. Grachev, K. Khodataev, A. Ravaev, N. Yurchenko, P. Vinogradsky, A. Zhdanov, “Initiated surface microwave discharge as an efficient active boundary-layer control method”, *AIAA Paper*, no. 2009-0889, 2009.
21. [Lebedev11] Yu.A. Lebedev, A.V. Tatarinov, I.L. Epshtein, “3D simulation of electrodynamics of a microwave low pressure discharge”, *High Temperature*, vol. 49, no. 6, pp. 775–787, 2011.
22. [Lebedev15]Yu.A. Lebedev, “Microwave discharges at low pressures and peculiarities of the processes in strongly non-uniform plasma”, *Plasma Sources Science and Technology*, vol. 24, no. 5, 053001, 2015.
23. [Kasimova18]S.R. Kasimova, “Improvement of the reflectivity of flat coatings”, *Journal of Engineering Physics and Thermophysics*, vol. 91, no 6, pp. 1592–1594, 2018.
24. [Esakov19]P.V. Denissenko, M.P. Bulat, I.I. Esakov, L.P. Grachev, K.N. Volkov, I.A. Volobuev, V.V. Upyrev, P.V. Bulat, “Ignition of premixed air/fuel mixtures by microwave streamer discharge”, *Combustion and Flame*, vol. 202, pp. 417-422, 2019.